Available online at www.sciencedirect.com
SCIENCE DIRECT
Polymer 46 (2005) 1157–1167
polymer
www.elsevier.com/locate/polymer

Characterization of colloidal polymer particles through stability ratio measurements

Andrea Vaccaro, Ján Šefčík, Massimo Morbidelli*

Swiss Federal Institute of Technology Zurich, Institut für Chemie-und Bioingenieurwissenschaften, ETH Hönggerberg/HCI, CH-8093 Zürich, Switzerland

Accepted 30 September 2004
Available online 8 December 2004

Abstract

We propose a general methodology for the estimation of the doublet formation rate constant (proportional to the stability ratio of primary particles) in colloidal dispersions from measurements obtained by common optical techniques, such as dynamic light scattering, static light scattering (nephelometry) or turbidimetry. In contrast to previous approaches relying on the initial slopes of the measured quantities, such as the mean hydrodynamic radius, scattered light intensity or turbidity, we introduce a transformation of the measurables to properly scaled quantities, which grow linearly in time with a slope proportional to the doublet formation rate. Analysis of systematic and random errors allows one to control the error in the estimated value of the aggregation rate. Using this approach, we measured the aggregation rate constant of colloidal polymer particles prepared by surfactant-free emulsion copolymerization of styrene and 2-hydroxyethyl methacrylate (HEMA). It was found that the stability ratio at constant ionic strength decreases with increasing dilution of the original polymer latex. This can be explained by the presence of non-reacted stabilizing species (most likely oxidized HEMA) that desorb from the particle surface upon latex dilution and thus diminish the repulsive interactions between particles. In order to check if the stability of latex particles is influenced by reversibly adsorbed species it is always necessary to perform aggregation experiments at various dilutions.

Keywords: Colloids; Aggregation; Kinetics

1. Introduction

Aggregation phenomena in colloidal dispersions are of great importance in many industrial processes, such as in polymer, food and pharmaceutical industries or in water treatment. In the production and handling of polymer latexes, it is crucial to control the coagulation kinetics in order to achieve colloidal stability. The primary particle aggregation or doublet formation rate constant is one of the fundamental characteristics of a colloidal dispersion and it is relevant for the quantitative understanding of the kinetics of aggregation and stability of colloidal particles. The doublet formation rate constant is used to derive the so-called Fuchs' stability ratio, which provides a direct quantitative measure of colloidal stability. The doublet formation rate constant is also the starting point for the formulation of aggregation kernels that allow modeling the time evolution of the particle size distribution in aggregating dispersions using population balance equations [1]. Consequently, the knowledge of the aggregation kinetics is a fundamental information for the efficient design and control of coagulation processes.

The stability ratio is controlled by interactions between primary particles due to dispersion, electrostatic, steric and other forces [2]. These interactions are strongly affected by the partitioning of various solutes, such as surfactants and salts, between the particle surface and the aqueous phase. It is therefore important to consider the adsorption and desorption behavior of water-soluble components in the latex when studying the colloidal stability of latex particles. For example, when a given latex is diluted with pure water to different solid volume fractions, various species originally present at the polymer particle surface can partially transfer to the aqueous phase according to their adsorption equilibria, thus affecting the colloidal stability. This process is well recognized in the literature and extensive latex cleaning procedures are recommended to remove soluble

* Corresponding author. Tel.: +41 16323034; fax: +41 16321082.
E-mail address: morbidelli@chem.ethz.ch (M. Morbidelli).

0032-3861/$ - see front matter © 2004 Elsevier Ltd. All rights reserved.
doi:10.1016/j.polymer.2004.11.058

components from the latex prior to aggregation kinetics measurements [3], in order to obtain primary particles that are stabilized exclusively by species irreversibly attached to the polymer surface. Another possibility to obtain a system with the same surface chemistry at various latex dilutions is to separate a mother liquor from a stock latex and to use it as the diluting medium.

The primary particle aggregation rate constant can be measured by a variety of methods, such as turbidimetry [4–7], Coulter counter [8,9], static light scattering (nephelometry) [10–12], dynamic light scattering [13–15] and combined multiangle static and dynamic light scattering [16]. All these methods are based on measuring certain physical quantities as a function of time during aggregation, estimating the initial rate of change of these quantities at times where the process is dominated by primary particle aggregation, and finally deriving from this the doublet formation rate by means of relationships that depend upon the specific physical quantity measured. The problem is the evaluation of the initial rate of change of the measured quantity, which often reduces to the estimation of the initial slope in a plot of experimental data disturbed by experimental error. In addition, it is not easy to identify a priori the maximum time value that can be considered before doublet aggregation becomes significant. In this work, we propose a procedure for estimating the doublet formation rate constant in aggregating colloidal dispersion of monodisperse spheres that overcomes these difficulties.

2. Measuring techniques

2.1. Static light scattering

Let us consider a colloidal dispersion of solid primary particles undergoing aggregation. The intensity of light scattered by a dilute sample can be expressed as follows:

$$I(q,t) = V_s \sum_i I_i(q) N_i(t), \tag{1}$$

where $I_i(q)$ and $N_i(t)$ are the intensity of light scattered by an aggregate containing i primary particles and its number concentration, respectively, V_s is the scattering volume and $q \equiv 4\pi n/\lambda_0 \sin(\theta/2)$ is the modulus of the scattering vector with n the refractive index of the suspending medium, λ_0 the wavelength of light in vacuo and θ the scattering angle.

Within the Rayleigh–Debye approximation [17], i.e. assuming that the electric field inside the particles is equal to that of the incident wave, the intensity scattered by an aggregate made up of i identical spherical particles can be expressed as follows

$$I_i(q) = A \quad I_0 \quad R_d^{-2} \quad i^2 S_i(q) P(q), \tag{2}$$

$$P(q) = \left[3 \frac{\sin(Rq) - Rq\cos(Rq)}{(Rq)^3} \right]^2,$$

$$S_i(q) = \frac{1}{i^2} \sum_{l,m} \frac{\sin(r_{lm} q)}{r_{lm} q},$$

where A is an optical constant, R_d is the distance between the scattering volume and the detector, I_0 is the intensity of the incident light, $P(q)$ is the form factor of the primary particles, $S_i(q)$ is the structure factor of the aggregate containing i primary particle and r_{lm} the distance between the centers of two primary particles belonging to the same aggregate.

2.2. Dynamic light scattering

Quasi-elastic or dynamic light scattering (DLS) experiments are based on the analysis of the temporal fluctuations of the scattered intensity due to the Brownian motion of the aggregates [18]. In a photocount homodyne experiment the measured quantity is the temporal autocorrelation function of the photocount rate

$$C(\tau) \equiv \langle n(0) n(\tau) \rangle, \tag{3}$$

here $\langle\ \rangle$ signifies an ensemble or infinite time average of the enclosed quantity, $n(t)$ is the count rate, i.e. the number photons hitting the detector in a time interval δt, and τ is the delay time. The most convenient way to calculate $C(\tau)$ is based on the scattered electric field ($E(\tau)$) correlation function

$$g^{(1)}(\tau) \equiv \frac{\langle \bar{E}(0) E(\tau) \rangle}{\langle |E(0)|^2 \rangle}, \tag{4}$$

where the overbar denotes the complex conjugate of the variable. Assuming that the fluctuating quantities are Gaussian stochastic variables, one can relate the measured correlation function $C(\tau)$ to $g^{(1)}(\tau)$ through the following relationship [19]

$$C(\tau) = \langle n \rangle^2 (1 + A' |g^{(1)}(\tau)|^2), \tag{5}$$

where $\langle n \rangle$ is the average count rate and A' is a constant of order one which depends on the detection optics and on the duration of the sampling time δt. In the case of monodisperse colloidal dispersions the modulus of the normalized first-order correlation function can be written as follows

$$|g^{(1)}(\tau)| = \exp(-\Gamma_i \tau), \tag{6}$$

where $\Gamma_i \equiv D_i q^2$ is the decay rate, with D_i the diffusion coefficient of the i-fold aggregate. More generally in an aggregating dispersion $|g^{(1)}(\tau)|$ is expressed in terms of a normalized distribution of decay rates G_i [20,21]

$$|g^{(1)}(\tau)| = \sum_i G_i \exp(-\Gamma_i \tau), \tag{7}$$

where

$$G_i = \frac{V_s I_i(q) N_i(t)}{V_s \sum_i I_i(q) N_i(t)} = \frac{i^2 S_i(q) N_i(t)}{\sum_i i^2 S_i(q) N_i(t)}. \quad (8)$$

Thus, once $|g^{(1)}(\tau)|$ is obtained from the experimentally measured photocount correlation function, through the previous relationships, useful information about particle diffusivities can be extracted by means of the method of cumulants [22]. The following MacLaurin expansion of $h(-\tau) \equiv \ln|g^{(1)}(\tau)|$

$$h(-\tau) = K_1(-\tau) + K_2 \frac{(-\tau)^2}{2!} + K_3 \frac{(-\tau)^3}{3!} + \cdots \quad (9)$$

defines the m-th cumulant K_m as $d^m h(-\tau)/d(-\tau)^m$ evaluated at $\tau = 0$. The most sensible information is contained in the first two terms K_1 and K_2 where the latter is related to the polydispersity of the particle size distribution, while the first one, calculated from the initial slope of the plot $\ln|g^{(1)}(\tau)|$ versus $-\tau$, represents the average decay rate weighted by G_i

$$K_1 = \bar{\Gamma} = \frac{\sum_i i^2 S_i(q) N_i(t) \Gamma_i}{\sum_i i^2 S_i(q) N_i(t)}. \quad (10)$$

By dividing both terms by q^2 we obtain the intensity weighted average of the diffusion coefficient

$$\bar{D} = \frac{\bar{\Gamma}}{q^2} = \frac{\sum_i i^2 S_i(q) N_i(t) D_i}{\sum_i i^2 S_i(q) N_i(t)}. \quad (11)$$

Often reported result of DLS measurements is the mean hydrodynamic radius resulting from the application of the Stokes–Einstein equation to the mean diffusivity

$$R_{DLS}(t, q) \equiv \frac{kT}{6\pi\mu\bar{D}} = \frac{\sum_i i^2 S_i(q) N_i(t)}{\sum_i i^2 S_i(q) N_i(t)/R_i^H}, \quad (12)$$

where $R_i^H \equiv kT/6\pi\mu D_i$ is the hydrodynamic radius of the i-fold aggregate. The equation shows that at the beginning of the aggregation process $R_{DLS}(0, q) = R_1^H = R$, since we have assumed the system to be monodisperse. Finally it is worth noting that R_{DLS} and R_i^H are simply radii of spheres whose diffusion coefficient is, in diluted conditions, equal to the average diffusivity $\bar{D}$, and the diffusivity of the i-fold cluster D_i, respectively. Only in the special case when all aggregates are spherical, e.g. due to coalescence, Eq. (12) can be rewritten in terms of the aggregate radii $R_i = R_i^H$, so that for $q \ll 1/\max\{R_i\}$ (i.e. point scatterers) R_{DLS} reduces to the following average radius

$$R_{DLS}(t) = R_{6,5}(t) \equiv \frac{\sum_i N_i(t) R_i^6}{\sum_i N_i(t) R_i^5}. \quad (13)$$

2.3. Turbidimetry

In turbidimetry the intensity I_t of the light transmitted by an incoherent monochromatic light beam impinging the sample is measured. Turbidity, which physically represents the sum of scattered and absorbed power per unit volume and per unit intensity of incident light, is then calculated through the relationship

$$\gamma = \frac{\log(I_0/I_t)}{l}.$$

where l is the length of the path traveled by the incident light. Turbidity can be related to the cluster number concentrations N_i through the total extinction cross-sections σ_i, which are defined as the power absorbed and scattered by the single cluster per unit intensity of incident light, in the following way

$$\gamma(t) = \sum_i N_i(t) \sigma_i. \quad (14)$$

Within the Rayleigh–Debye approximation and assuming that absorption phenomena can be neglected, i.e. that the refractive index of the solid phase has zero imaginary part, the total extinction cross-section for the i-fold aggregate is [17]

$$\sigma_i = \sigma_i^s = 2\pi A i^2 \int_0^\pi \frac{1 + \cos^2\theta}{2} S_i(\theta) P(\theta) \sin\theta \, d\theta,$$

where σ_i^s is the total scattering cross-section of the i-fold cluster, A is the same optical constant as in Eq. (2), and the structure and form factors are also the same but expressed in terms of the scattering angle θ instead of q. We note that the term $(1 + \cos^2\theta)/2 < 1$ arises from the non-coherency of the incident light.

3. Estimation of primary particle aggregation rate

3.1. Aggregation kinetics

In colloidal dispersions particles collide due to Brownian motion and aggregate because of attractive dispersion forces. Aggregation kinetics can be modeled by the population balance equation (Smoluchowski coagulation equation), written for the i-fold aggregate as:

$$\frac{dN_i(t)}{dt} = \frac{1}{2} \sum_{l+m=i} K_{lm} N_l(t) N_m(t) - N_i(t) \sum_{j=1}^{\infty} K_{ij} N_j(t), \quad (15)$$

where N_i is the number concentration of the i-fold aggregate, while $\{K_{lm}\}$ is the aggregation kernel which represents the matrix of second-order rate constants of aggregation between a l-fold aggregate and a m-fold aggregate and contains the entire information about the physics of the aggregation mechanism. This means that the aggregation kinetics can be quantitatively described when an appropriate formulation for $\{K_{lm}\}$ is provided. Since the present work is mainly concerned with doublet formation rate we will focus our attention only on one element of $\{K_{lm}\}$, namely K_{11}.

The simplest model of aggregation is obtained in absence

of interparticle interactions where doublet formation is controlled by Brownian diffusion [23]:

$$K_{11} = K_B = \frac{8kT}{3\mu}, \tag{16}$$

where k is the Boltzmann constant, T is the temperature and μ the viscosity of the continuous phase.

In the more realistic situation where interparticle interactions are present, one obtains [2]

$$K_{11} = \frac{K_B}{W}, \tag{17}$$

$$W \equiv 2\int_2^\infty \frac{\exp\left(\frac{U(\xi)}{kT}\right)}{G(\xi)\xi^2}\mathrm{d}\xi, \quad \xi \equiv \frac{r}{R}, \tag{18}$$

where R is the particle radius, r is the interparticle distance, $U(\xi)$ is the particle interaction potential, and the term $G(\xi)$ accounts for the hydrodynamic resistance due to fluid outflow upon the mutual approach of two particles. W is the Fuchs' stability ratio, and its inverse is equal to the ratio between the primary particle aggregation rate and its theoretical value in the absence of interparticle interactions.

3.2. Early stage aggregation: scaled quantities

Here we consider the early stages of the aggregation process where we can assume that only primary particles and doublets are present. Under this assumption Eq. (15) leads to:

$$N_1(t) = \frac{N}{1 + t/\tau_a}; \quad N_2(t) = \frac{N}{2}\frac{t/\tau_a}{1 + t/\tau_a}, \tag{19}$$

with $N \equiv N_1(0)$ denoting the initial number concentration of primary particles and $\tau_a \equiv (K_{11}N)^{-1}$ the characteristic time of aggregation. These relationships are asymptotically accurate at short times when the rate of doublet consumption is small compared to the rate of its formation, i.e.

$$\frac{K_{12}N_1(t)N_2(t)}{\frac{1}{2}K_{11}N_1(t)^2} \ll 1.$$

Using Eq. (19) and considering that K_{12} and K_{11} are of the same order of magnitude the relation above leads to

$$\frac{2N_2(t)}{N_1(t)} = t/\tau_a \ll 1, \tag{20}$$

which provides a quantitative estimate of the time interval where Eq. (19) can be applied. Now, substituting Eq. (19) in Eq. (12) and scaling by the primary particle radius, we get

$$R^*_{DLS}(t,q) \equiv \frac{R_{DLS}(t,q)}{R} = \frac{1 + 2S_2(q)t/\tau_a}{1 + 2(S_2(q)t/\tau_a)R/R_2^H}, \tag{21}$$

where the doublet structure factor is $S_2(q) = 1/2[1 + \sin(2Rq)/(2Rq)]$ and the hydrodynamic radius of the doublet R_2^H has been obtained from its diffusivity, which in the case of two touching solid primary particles gives $R_2^H \simeq 1.38R$ [16].

Applying the same procedure to turbidity and scattered intensity, starting from Eqs. (14) and (1), respectively, we obtain

$$\gamma^*(t) \equiv \frac{\gamma(t)}{\gamma(0)} = \frac{1 + \frac{\sigma_2}{2\sigma_1}(t/\tau_a)}{1 + t/\tau_a}, \tag{22}$$

$$I^*(q,t) \equiv \frac{I(q,t)}{I(q,0)} = \frac{1 + 2S_2(q)(t/\tau_a)}{1 + t/\tau_a}. \tag{23}$$

Once the radius of the primary particle R and the characteristic time of aggregation τ_a are known, the time evolution of the measured hydrodynamic radius, non-dimensional turbidity and non-dimensional intensity can be predicted, within the time interval where condition (20) remains valid, using Eqs. (21)–(23), respectively.

It is now convenient to rearrange Eqs. (21)–(23) in order to obtain linear relationships in time:

$$\varrho_{DLS}(t,q) \equiv \frac{1}{2S_2(q)}\frac{R^*_{DLS}(t,q) - 1}{1 - \alpha R^*_{DLS}(t,q)} = K_{11}Nt, \tag{24}$$

$$\varrho_\gamma(t) \equiv \frac{\gamma^*(t) - 1}{\frac{\sigma_2}{2\sigma_1} - \gamma^*(t)} = K_{11}Nt, \tag{25}$$

$$\varrho_I(t,q) \equiv \frac{I^*(q,t) - 1}{2S_2(q) - I^*(q,t)} = K_{11}Nt, \tag{26}$$

where $\alpha \equiv R/R_2^H = 1/1.38$, $\sigma_2/2\sigma_1$ can be obtained from Fig. 1 if the Rayleigh–Debye approximation condition [17] is met and $\varrho_{DLS}(t,q)$, $\varrho_\gamma(t)$ and $\varrho_I(t,q)$ are defined as scaled hydrodynamic radius, turbidity and intensity, respectively, and can be computed from the corresponding quantity measured experimentally (i.e. hydrodynamic radius, turbidity or scattered light intensity) and the primary particle radius, R. It is important to note that based on Eq. (20) the above equations strictly apply for

$$\varrho_{DLS}(t,q) \ll 1, \quad \varrho_\gamma(t) \ll 1, \quad \varrho_I(t,q) \ll 1. \tag{27}$$

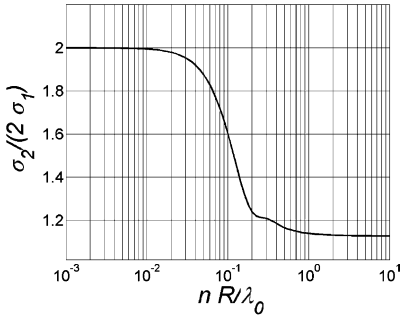

Fig. 1. Plot of the ratio between the scattering cross-section of the doublet and the double of the scattering cross-section of the monomer versus the non-dimensional length scale nR/λ_0.

Thus, during an aggregation experiment we measure one of the relevant quantities mentioned above as a function of time, and we plot the corresponding scaled quantity versus time using Eqs. (24), (25) or (26). If in the initial region we obtain a straight line, then its slope is equal to $K_{11}N$. Note that such a straight line is certainly obtained in the region where condition (27) is satisfied. However, this can extend also to larger ϱ even in the case where Eq. (20) is not valid, as for example if the doublets are less reactive than the primary particles.

3.3. Accuracy assessment of the estimation procedure

The analysis above indicates that in order to minimize the systematic error in the estimate of K_{11} due to the aggregation of doublets, the measurement time should be sufficiently short, i.e. $t \ll \tau_a$. On the other hand, we have to consider that every analytical technique has an instrumental random error, and therefore we need a sufficient duration of the experiment in order to be able to collect enough measurements to reduce the effect of such error on the obtained estimate of K_{11}. Let us look at the instrumental error in more detail. Let σ_{DLS} be the standard deviation of the hydrodynamic radius measurement R_{DLS}, then standard error analysis tells us that, starting from Eq. (24), the standard deviation σ_ϱ of the scaled hydrodynamic radius can be expressed as follows

$$\sigma_\varrho = \frac{(1-\alpha)\sqrt{1+\left(\frac{R_{DLS}}{R}\right)^2}}{2S_2(q)R\left(1-\alpha\frac{R_{DLS}}{R}\right)^2}\sigma_{DLS}.$$

If we collect n_p measurements at times $t_j = jt_{meas}$, where t_{meas} is the single measurement duration, then the slope K estimated through linear interpolation (passing through the origin of coordinates, i.e. $\varrho_{DLS} = 0$ at $t = 0$) of the scaled radii $\varrho_{DLS,j} = \varrho_{DLS}(t_j, q)$ and the corresponding standard deviation σ_K take this form

$$K = \frac{\sum \varrho_{DLS,j} t_j/\sigma^2_{\varrho,j}}{\sum t_j^2/\sigma^2_{\varrho,j}},$$

$$\sigma_K = \frac{1}{\sqrt{\sum t_j^2/\sigma^2_{\varrho,j}}},$$

where $\sigma_{\varrho,j}$ is given by the previous formula evaluated at t_j. As the number of measurements n_p increases the standard deviation of the measured slope decreases until a certain number of experimental points n_p^* is reached where the decrease is not significant anymore. Based on this observation alone, one would want to decrease the measurement duration t_{meas} in order to increase the number of measurements in a given observation time. Yet, as for the standard deviation of the estimated slope, when a certain minimum value t^*_{meas} is reached the instrumental error of the single measurement σ_{DLS} will start to increase significantly. This means that the best measurement setup yielding the minimum instrumental error in the shortest observation time is obtained when performing n_p^* measurements each of duration t^*_{meas}.

However, as discussed above, the observation time has to satisfy the constraint (27), in order to avoid the significant formation of triplets. If this were not the case then a systematic error would be introduced, leading to an overestimation of K_{11} and thus an underestimation of the stability ratio. Consequently, for each experimental condition an optimal measurement setup exists that minimizes the sum of instrumental and systematic error.

This is illustrated in Fig. 2(a) and (b) where the systematic and instrumental errors are shown together with their sum for a simulated typical example. In Fig. 2(a) the relative errors are plotted as a function of the number of measurements taken at constant measurement frequency (8.6 per unit τ_a). In Fig. 2(b) the relative errors have been plotted as a function of the measurement frequency with constant number of measurements (equal to 4). The simulated experimental data on aggregation kinetics were generated by numerically solving Eq. (15) with the constant kernel [24]. The standard deviation for DLS measurements

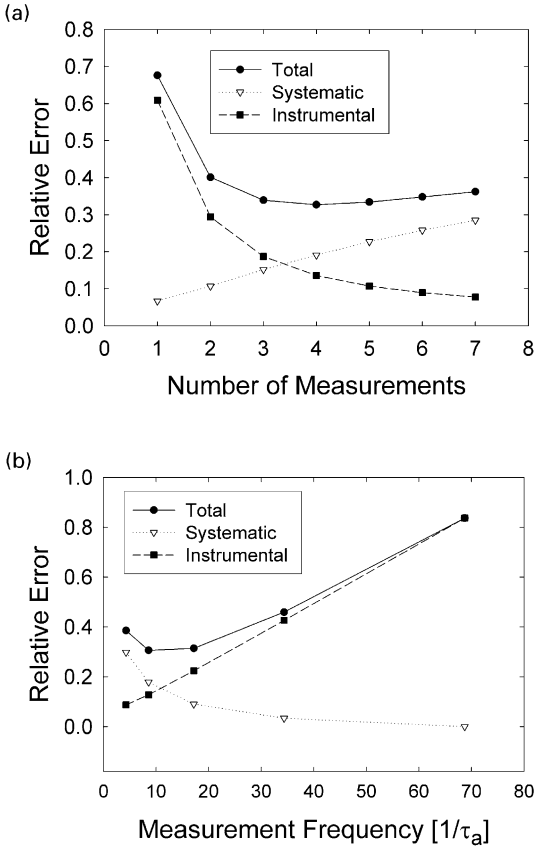

Fig. 2. Relative error in estimated value of the stability ratio for a simulated experiment as function of: (a) the number of measurements with constant frequency (8.6 measurement per unit τ_a), (b) the measurement frequency with total number of measurements equal to 4.

was assumed, for the sake of illustration, to be 2.6% of the hydrodynamic radius. However, when considering a particular measurement the standard deviation should be estimated based on experimental data. The instrumental error was calculated by means of the formulas previously presented while the systematic error was computed as difference between the K_{11} value estimated through linear interpolation and the theoretical value used to simulate the experimental data. The calculated theoretical relative errors are independent of the actual values of K_{11} or N.

It can be seen that as the experiment duration increases the systematic error increases, while the instrumental one decreases. This indicates that there are conditions where the total relative error is minimized and so the best estimate of K_{11} can be obtained, when we accept a certain systematic error introduced by the inaccuracy of the simplified kinetic scheme, while achieving a considerably lower instrumental error.

The above theoretical error analysis can also be applied for static light scattering and turbidimentry, using the corresponding functional forms of scaled quantities. However, these techniques provide faster measurements with less fluctuations compared to DLS, so that smaller instrumental errors can be expected and shorter times can be used for measurements.

4. Experimental section

4.1. Materials and instruments

An emulsifier-free polymer latex was prepared by emulsion copolymerization of styrene (Fluka, purity ≥ 99%) and 2-hydroxyethyl methacrylate (HEMA) (Fluka, purity ≥ 99%) [25] following the polymerization recipe reported in Table 1. Potassium persulfate (KPS) (purity ≥ 99%) was used as initiator. The reaction was carried out in a 0.5 l jacketed reactor under nitrogen atmosphere at a stirring speed of 350 rpm until 92.1% weight conversion was reached after about 20 h. Table 2 summarizes the relevant properties of the final dispersion.

Solid content was measured by gravimetry (HG53 Halogen Moisture Analyzer, Mettler Toledo). Throughout all the experiments water was distilled twice and then filtered through a Millipore equipment. Sodium chloride (Fluka, Analytical Grade) was used to induce aggregation. DLS measurements were performed with an argon-ion laser M95-2 (Lexel) at 25 °C using a BI-200SM goniometer (Brookhaven) at the scattering angle of 50°.

Table 2
Dispersion properties

Solid volume fraction (%)	DLS diameter (nm)	Particle concentration (m^{-3})
9.0	84	3.45×10^{19}

4.2. The aggregation experiment

Aggregation in electrostatically stabilized colloidal dispersion is typically induced by the addition of an electrolyte, which screens the surface charges of the primary particles. Thus a typical aggregation experiment requires mixing of a colloidal dispersion with an electrolyte solution. This operation requires some comments since it may lead to significant experimental errors in aggregation kinetics measurements.

The aggregation process is in fact controlled by two characteristic times: the characteristic time of mixing τ_m and the characteristic time of aggregation τ_a. In order to measure the true aggregation rate at the chosen electrolyte concentration we need to fulfill two requirements. First, the aggregation process should take place at uniform conditions in the entire vessel, which requires the mixing time to be much shorter than the aggregation time, i.e. $\tau_m \ll \tau_a$. Second, the aggregation itself should have a duration compatible with appropriate monitoring. However, in some conditions these two requirements may contradict each other.

When a volume V_S of the electrolyte solution is mixed with a volume V_D of the colloidal dispersion, local overshoots in both particle and electrolyte concentrations are experienced in the system before homogeneity is achieved ($t < \tau_m$). This might result in a significant extent of uncontrolled, and therefore undesired, aggregation. The concentration overshoots can be quantified by writing the following balances on particle and electrolyte concentrations, respectively

$$N = \frac{V_D}{V_D + V_S} N_D \tag{28}$$

$$I = \frac{1-\phi_D}{1-\phi}\frac{V_D}{V_D+V_S} I_D + \frac{1}{1-\phi}\frac{V_S}{V_D+V_S} I_S, \tag{29}$$

here N is the particle number concentration, $\phi = 4/3\pi R^3 N$ is the solid volume fraction and $I \equiv 1/2 \sum_i z_i^2 c_i$ is the ionic strength in the final dispersion with z_i and c_i being the charge and the concentration of the i-th electrolyte, respectively. Subscripts D and S relate to the initial colloidal dispersion

Table 1
Polymerization recipe

Styrene (g)	HEMA (g)	KPS (mg)	Water (g)	Temperature (°C)
45.3	3.35	500	450	75

and salt solution, respectively, while no subscript refers to the final composition.

Let us first consider the case of ionic strengths above the critical coagulation concentration (CCC) in the diffusion limited regime, where the aggregation rate constant K_{11} is independent on the electrolyte concentration. In such conditions K_{11} is on the order of 10^{-17} m^3/s for aqueous solutions so that in order to conveniently monitor aggregation kinetics, we have to work at very low particle number concentrations N. For example, given a typical number concentration of a stock latex dispersion $N_D \approx 10^{21}$ m^{-3}, in order to achieve $\tau_a = (K_{11}N)^{-1} \simeq 2$ h, the dilution factor should be on the order of 10^{-8}. Such dilution can be achieved either by taking the stock dispersion and diluting it with a salt solution to the target salt and particle concentrations or by prediluting the original dispersion with water to a particle concentration N_D very close to the desired N and then adding a small volume of a concentrated salt solution. In the first case, the particle concentration overshoot occurs in the course of mixing and therefore it leads to undesired aggregation. In the second case, the salt overshoot takes place near the desired particle concentration but, since we are above the CCC, this overshoot in salt concentration does not affect the aggregation rate, thus allowing the experiment to take place at the desired conditions.

Now let us consider the case of aggregation experiment at ionic strength values substantially lower than the CCC, in this situation the salt concentration overshoot, proportional to $(I_s - I)$, must be minimized due to the extreme sensitivity of K_{11}on this quantity [2]. On the other hand, since the value of K_{11} is small, we need sufficiently large particle concentrations N in order to have a reasonable experiment duration. If we solve Eqs. (28) and (29) for $I_s - I$ we get

$$I_S - I = \frac{N}{N_D - N}(1 - \phi_D)(I - I_D), \tag{30}$$

which indicates that in order to minimize this difference one has to decrease N and increase N_D. However, as seen above, there is a lower limit for the particle number concentration in the aggregating dispersion N while an upper limit for N_D is imposed by the particle concentration in the stock colloidal dispersion $\bar{N}_D$. Thus the minimum attainable overshoot is:

$$I_S - I = \frac{N}{\bar{N}_D - N}(1 - \bar{\phi}_D)(I - \bar{I}_D), \tag{31}$$

where $\bar{\phi}_D$ and $\bar{I}_D$ are the dispersion particle volume fraction and ionic strength in the stock colloidal dispersion, respectively, and N is the minimum value leading to a maximum tolerable aggregation timescale $\tau_a = 1/K_{11}N$. Note that this analysis implies that the lower is the target ionic strength, the smaller will be K_{11}, consequently the higher will be N and the larger will be the ionic strength overshoot, thus indicating that for any given colloidal system there exists a minimum salt concentration below which the doublet formation rate constant cannot be measured.

As discussed above, the relative amount of salt solution and latex as well as the corresponding concentrations and mixing procedure, have to be carefully selected for each aggregation experiment so as to minimize overshoots in salt and particle concentrations, and to obtain a reasonably short duration of the aggregation experiment where, however, the relevant part, i.e. $t < \tau_a$, should be sufficiently long to take proper measurements. In order to perform on-line DLS measurements substantial dilutions of the stock latex were required. To reduce the experimental error this was done in two dilution steps with water. Care was taken that the particle number concentration of the obtained dispersion was high enough to avoid salt overshoots in the last mixing step with the salt solution. Indeed in every experiment the salt concentration in the salt solution used to induce aggregation in the last step was always very near to the target salt concentration. Experiments were carried out in 20 ml glass beakers which were carefully washed and extensively rinsed with distilled water. Throughout sample preparation and its successive handling any dust contamination was carefully avoided.

5. Results and discussion

Aggregation experiments were performed at three different dilution factors f of the original latex while keeping the remaining experimental parameters fixed as detailed in Table 3. Each experiment consisted of four to six runs, so as to estimate mean values and standard deviations of the latex stability ratio W as a function of the latex dilution factor f, and the corresponding polymer volume fraction, ϕ.

Fig. 3(a) shows a typical measurement in terms of time evolution of the mean hydrodynamic radius for the run A1 corresponding to the experimental conditions A in Table 3.

Once the evolution of the hydrodynamic radius over a period of time was measured, the corresponding values of the scaled radius ϱ_{DLS} were computed through Eq. (24) and plotted as a function of time, as shown in Fig. 3(b) for the data in Fig. 3(a). Shortly after $\varrho_{DLS}(t, q)$ passes unity, which implies that time is of the order of τ_a, a more-than-linear growth becomes evident. This is due to the occurrence of significant doublet aggregation that has been neglected in deriving Eq. (24). The scaled radius $\varrho_{DLS}(t, q)$ in fact diverges for $R_{DLS}(t, q) = R_2^H$, condition that in the above simplified kinetic treatment is reached only at infinitely long times.

In Fig. 4 we show the evolution of the scaled radius at the early stages of aggregation where it exhibits a region of linear behavior in time. From the linear fit of the data in Fig. 4 according to $\varrho_{DLS}(t, q) = K_{11}Nt$ we estimate the doublet formation rate constant K_{11} as the particle number

Table 3
Operating conditions in the aggregation experiments

Exp.	I (mM)	ϕ ($\times 10^5$)	N ($\times 10^{-16}$ m^{-3})	f	W ($\times 10^3$)	Std. dev. ($\times 10^3$)
A	225	8.56	3.45	1000	1.4	0.59
B	225	2.57	1.03	3333	0.58	0.21
C	225	0.856	0.345	10,000	0.30	0.063

concentration N is known. Note that the linearity region extends to ϱ values which are relatively close to one. In our experience with polymer latexes we have observed that this is often the case, thus indicating that the condition $\varrho \ll 1$ is too restrictive as discussed in the context of Eq. (27).

The estimated values of K_{11} together with the corresponding standard deviations are summarized in Table 3 in terms of stability ratios $W = K_B/K_{11}$. It is seen that the stability ratio W tends to decrease with increasing dilution factor f. However, this trend appears to be weak since the confidence intervals on W are rather wide. Such scatter of the experimental data is not unusual for colloidal aggregation experiments and may be related to irreproducible desorption of small amounts of species from the polymer particle surface upon latex dilution, in addition to the well known sensitivity of the stability ratio to the solution ionic strength. On the other hand, the decreasing of colloidal stability with increasing latex dilution at a given ionic strength is not expected for nominally surfactant-free latexes as those considered in this work. Instead, in the presence of ionic surfactants this behavior would be justified by the desorption of surfactants upon dilution which leads to a decrease of the colloidal stability. This suggests that some surface active species might be nevertheless present in our latex owing to the peculiarities of the polymerization reaction.

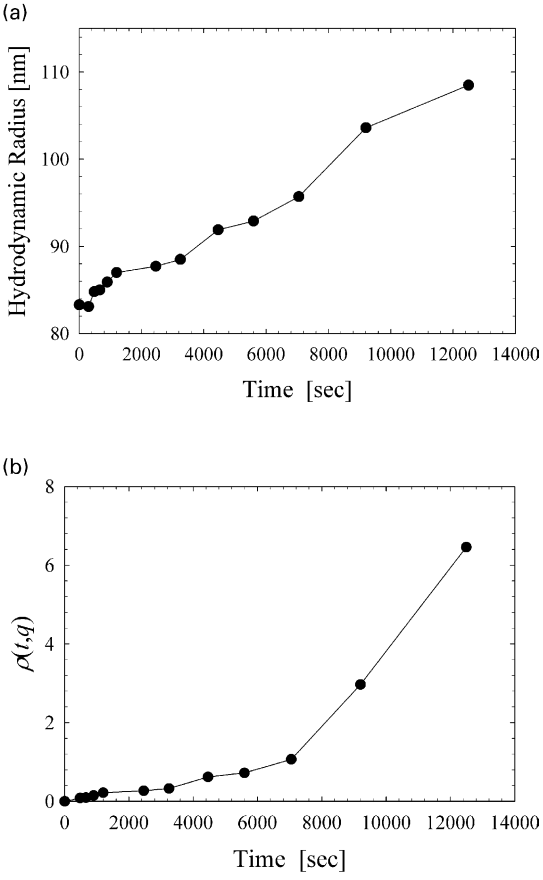

Fig. 3. (a) Hydrodynamic radius as a function of time for a run corresponding to the experimental condition A in Table 3. (b) Scaled radius as a function of time for the same runs as in (a).

In the first stage of styrene-HEMA emulsion copolymerization particles are homogenously nucleated (i.e. with no surfactant) [25,26]. Surface characterization studies [27,28] showed the presence of both strong and weak acid groups on the polymer particle surface. Strong acid sites are due to the sulphonate groups originating from the initiator. Weak acid sites result from the oxidation [29,28,30] of HEMA alcoholic function by persulphate, which is a strong oxidizing agent. Since the same process occurs also for the unreacted HEMA in solution we should expect the presence of weak acid groups also in the suspending medium. Since these molecules might effectively act as surfactants this could explain the observed effect of latex dilution on latex stability. In order to assess the magnitude of this effect we modeled the evolution of the emulsion copolymerization reaction with conversion (see Appendix A for details). Results corresponding to our experimental conditions are shown in Fig. 5. Fig. 5(a) shows the weight conversion of each monomer (Y_1 for styrene and Y_2 for HEMA) as a function of the overall weight conversion. It is seen that HEMA is less reactive, that is, it adds more slowly to the polymer than styrene, resulting in a smaller final conversion at overall final conversion $X_f = 0.921$. The net result is that a fraction of HEMA greater than styrene is left unreacted and partitioned between polymer particle surface

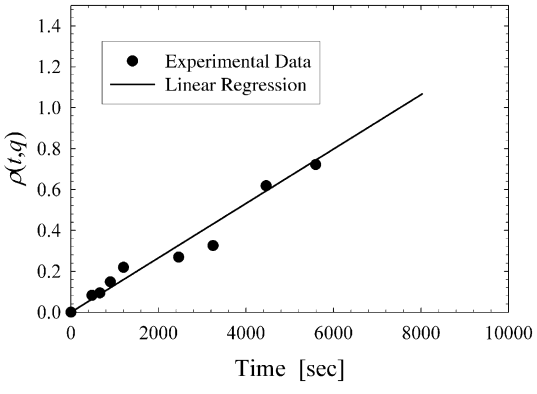

Fig. 4. Linear regression over the linear regime in Fig. 3(b).

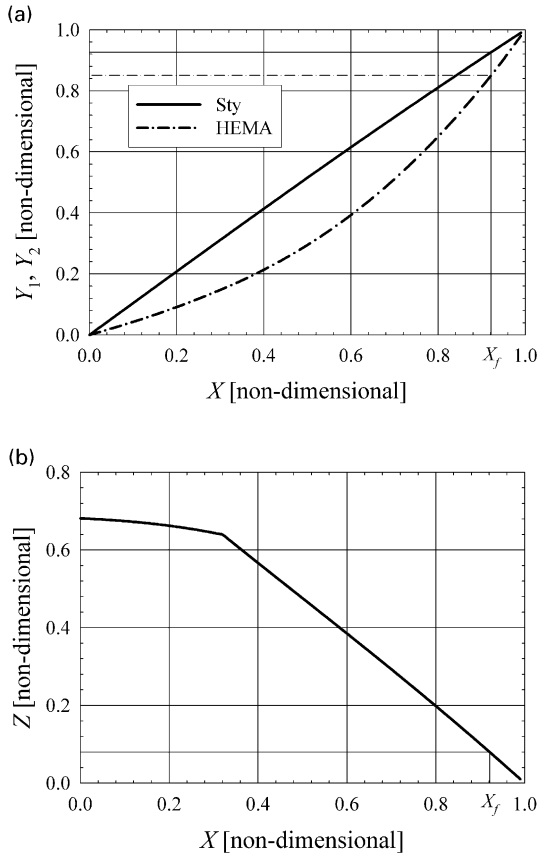

Fig. 5. (a) Monomer weight conversion as a function of overall weight conversion. (b) Ratio between the mass of HEMA dissolved in water and its total initial amount as a function of weight conversion.

and the aqueous phase. Fig. 5(b) illustrates this phenomenon by showing the ratio Z between the mass of HEMA dissolved in water and its total initial amount. The results show that at the final conversion, X_f almost 8% of the initial HEMA is present unreacted in the latex.

Returning to the interpretation of the measured stability ratios, we have shown that there is a substantial amount of unreacted HEMA left in the latex at the end of the polymerization. The unreacted HEMA has been likely oxidized to a weak acid which might act as a surfactant desorbing or adsorbing at the polymer particle surface upon changes in the latex solid volume fraction. This supports the proposed explanation that the observed decrease in colloidal stability with increasing dilution is due to the desorption of species, most likely the oxidized HEMA, which have a stabilizing effect on the polymer dispersion.

6. Conclusions

Aggregation kinetics of colloidal particles is commonly monitored by optical techniques such as dynamic light scattering, nephelometry or turbidimetry. In this work we have introduced a general procedure for the reliable estimation of the doublet formation rate constant or the corresponding stability ratio from measurements collected by any of the above techniques. In order to avoid the estimation of the initial slope of the plot of a measured quantity versus time, we propose a transformation of variables that leads to the definition of a scaled quantity which is expected to grow linearly in time, over a certain interval of time. The slope of the straight line interpolating the transformed experimental data in this interval yields an estimate of the doublet formation rate constant, while a deviation from the linear behavior indicates when doublet aggregation becomes significant or that the stability ratio changes in time. Analysis of systematic and random errors in the case of dynamic light scattering allows us to control the error in the estimated value of the stability ratio.

We applied the proposed procedure to the measurement of the aggregation kinetics of primary particles in a styrene-HEMA latex prepared by surfactant-free emulsion copolymerization and diluted to various solid volume fractions. Although the latex is nominally surfactant-free, the stability ratio of the primary particles was found to decrease with latex dilution at a constant ionic strength. This was attributed to the presence of stabilizing species, most likely originating from the oxidation of non-reacted HEMA in the original latex.

Appendix A. Sty-HEMA emulsion copolymerization modelling [31,32]

At a given overall conversion value, X, the material balances on styrene (monomer 1) and HEMA (monomer 2) are as follows

$$M_1^0 - Y_1 X(M_1^0 + M_2^0) = M_1^{\mathrm{m}} + V_{\mathrm{p}}\phi_1\rho_1, \tag{A1}$$

$$M_2^0 - Y_2 X(M_1^0 + M_2^0) = V_{\mathrm{m}}\alpha_2\rho_2 + V_{\mathrm{w}}c_2^{\mathrm{w}} + V_{\mathrm{p}}\phi_2\rho_2, \tag{A2}$$

where c_2^{w} is the weight concentration of HEMA, M_1^0 and M_2^0 represent the initial amount in mass of monomer 1 and 2, respectively, M_1^{m} the mass of styrene in the monomer phase, V_{m}, V_{p} and V_{w} the volumes of the monomer, particle and water phases, respectively, ρ_i the density of monomer i, and α_i and ϕ_i the volume fraction of the i-th monomer in monomer and particle phase, respectively. Weight conversion and polymer weight compositions are defined as follows

$$X \equiv \frac{M_1^0 + M_2^0 - (M_1 + M_2)}{M_1^0 + M_2^0},$$

$$Y_1 \equiv \frac{M_1^0 - M_1}{M_1^0 + M_2^0 - (M_1 + M_2)}, \tag{A3}$$

$$Y_2 \equiv \frac{M_2^0 - M_2}{M_1^0 + M_2^0 - (M_1 + M_2)},$$

where M_1 and M_2 represent the mass of styrene and HEMA at a conversion X, respectively. Furthermore phase volumes can be expressed as follows

$$V_p = \frac{X(M_1^0 + M_2^0)}{\rho_p}\frac{1}{\phi_p},$$

$$V_w = \frac{M_w^0}{\rho_w(1 - c_2^w)},$$

$$V_m = \frac{M_1^m}{\rho_1 \alpha_1},$$

where ϕ_p is the volume fraction of polymer in the particles, M_w^0 the mass of water and ρ_w its density, while the polymer density ρ_p is expressed as follows

$$\rho_p = \frac{Y_1 MW_1 + Y_2 MW_2}{Y_1 V_1 + Y_2 V_2},$$

where V_i are molar volumes and MW_i the molecular weights of the monomers.

Under the assumptions of (*i*) equiripartition between the two organic phases [33], and (*ii*) constant maximum swelling [34] the following partitioning equations apply:

$$\frac{\phi_1}{\phi_2} = \frac{\alpha_1}{\alpha_2}, \tag{A4}$$

$$\phi_p = 0.335, \tag{A5}$$

$$c_2^w = \frac{\phi_2 \rho_2}{H_2},$$

where H_2 is defined as the partitioning coefficient for HEMA between the monomer phase and water. It is important to note that the equations above are valid as long as the monomer phase is present, that is when $M_1^m \geq 0$. In the absence of the monomer phase, the first terms in the right hand side of Eqs. (A1) and (A2) drop out and Eqs. (A4) and (A5) become not relevant.

Differentiation of Y_1 as expressed in Eq. (A3) with respect of X after some rearrangements yields the following expression

$$\frac{dY_1}{dX} = \frac{Y_1}{X} - \frac{f_1}{X},$$

where $f_1 \equiv dM_1/d(M_1 + M_2)$ is obtained from the instantaneous monomer mass balances. In particular, introducing appropriate expressions for the kinetics of the relevant reactions and using the quasi steady state assumption, we obtain:

$$f_1 = \frac{\frac{V_2}{V_1} r_1 \phi_1^2 + \phi_1 \phi_2}{\frac{V_2}{V_1} r_1 \phi_1^2 + \frac{MW_1 + MW_2}{MW_1}\phi_2 \phi_2 + \frac{V_1 MW_2}{V_2 MW_1} r_2 \phi_2^2}, \tag{A6}$$

where r_i are the reactivity ratios.

Upon proper simplifications and rearrangements the final model equations are obtained as follows

$$\frac{dY_1}{dX} = \frac{Y_1}{X} - \frac{\frac{V_2}{V_1} r_1 \phi_1^2 + \phi_1 \phi_2}{\frac{V_2}{V_1} r_1 \phi_1^2 + \frac{MW_1 + MW_2}{MW_1}\phi_2 \phi_2 + \frac{V_1 MW_2}{V_2 MW_1} r_2 \phi_2^2}\frac{1}{X}, \tag{A7}$$

with:

$$M_1^m = M_1^0 - Y_1 X(M_1^0 + M_2^0) - V_p \phi_1 \rho_1, \tag{A8}$$

$$M_2^0 - Y_2 X(M_1^0 + M_2^0) = V_m \alpha_2 \rho_2 + V_w c_2^w + V_p \phi_2 \rho_2, \tag{A9}$$

$$V_p = \frac{X(M_1^0 + M_2^0)(Y_1 V_1 + Y_2 V_2)}{(Y_1 MW_1 + Y_2 MW_2)\phi_p}, \tag{A10}$$

$$V_w = \frac{M_w^0}{\rho_w(1 - c_2^w)}, \quad V_m = \frac{M_1^m}{\rho_1(1 - \alpha_2)},$$

$$\alpha_2 = \frac{\phi_2}{1 - \phi_p}, \quad \phi_1 = 1 - \phi_p - \phi_2, \tag{A11}$$

$$c_2^w = \frac{\phi_2 \rho_2}{H_2}, \quad Y_2 = 1 - Y_1,$$

for $X \leq (M_1^0 - V_p \phi_1 \rho_1)/(Y_1 X(M_1^0 + M_2^0))$ and

$$M_2^0 - Y_2 X(M_1^0 + M_2^0) = V_w c_2^w MW_2 + V_p \phi_2 \rho_2, \tag{A12}$$

Table A1
Parameter values used in the simulation of the STY (1) HEMA (2) copolymerization

Parameter	Value	Units	Reference
V_1	115	ml/mol	
V_2	121	ml/mol	
MW_1	104.2	g/mol	
MW_2	130.1	g/mol	
M_1^0	45.3	G	
M_2^0	3.35	G	
M_w^0	270	G	
H	1.62	–	[35]
ρ_1	0.906	g/ml	
ρ_2	1.071	g/ml	
ρ_w	1	g/ml	
r_1	0.53	–	[36]
r_2	0.59	–	[36]

$$V_p = \frac{X(M_1^0 + M_2^0)(Y_1V_1 + Y_2V_2)}{(Y_1MW_1 + Y_2MW_2)\phi_p},$$
$$V_w = \frac{M_w^0}{\rho_w(1 - c_2^w)}, \quad (A13)$$

$$\phi_1 = 1 - \phi_p - \phi_2, \quad c_2^w = \frac{\phi_2\rho_2}{H_2}, \quad Y_2 = 1 - Y_1, \quad (A14)$$

for $X \geq (M_1^0 - V_p\phi_1\rho_1)/(Y_1X(M_1^0 + M_2^0))$.

Eq. (A8) (or Eq. (A12) when applicable) provide ϕ_1 and ϕ_2 in terms of Y_1, which in turn is used to integrate Eq. (A7) backwards in conversion with initial condition $Y_1(X = 1) = M_1^0/(M_1^0 + M_2^0)$. The values of the parameters used in the simulations shown in Fig. 5 are reported in Table A1.

References

[1] Ramkrishna D, Mahoney AW. Chemical Engineering Science 2002; 57(4):595–606.
[2] Russel WB, Saville DA, Schowalter WR. Colloidal Dispersions. Cambridge: Cambridge University Press; 1989.
[3] Wilkinson MC, Hearn J, Steward PA. Adv Colloid Interface Sci 1999; 81(2):77–165.
[4] Lichtenbelt JWTh, Ras HJMC, Wiersema PH. J Colloid Interface Sci 1974;46(3):522–7.
[5] Lichtenbelt JWTh, Pathmamanoharan C, Wiersema PH. J Colloid Interface Sci 1974;49(2):281–5.
[6] Maroto JA, de las Nieves FJ. Colloid Polym Sci 1997;275(12): 1148–55.
[7] Puertas AM, de las Nieves FJ. J Phys—Condensed Matter 1997;9(16): 3313–20.
[8] Broide ML, Cohen RJ. J Colloid Interface Sci 1992;153(2):493–508.
[9] Matthews BA, Rhodes CT. J Colloid Interface Sci 1970;32:332.
[10] Lips A, Smart C, Willis E. Trans Faraday Soc 1971;67(586):2979–88.
[11] Lips A, Willis E. Trans Faraday Soc 1972;69:1226–36.
[12] Van Zanten JH, Elimelech M. J Colloid Interface Sci 1992;154(1): 1–7.
[13] Virden JW, Berg JC. J Colloid Interface Sci 1992;149(2):528–35.
[14] Herrington TM, Midmore BR. J Chem Soc, Faraday Trans 1 1989; 85(10):3529–36.
[15] Barringer EA, Novich BE, Ring TA. J Colloid Interface Sci 1984; 100(2):584–6.
[16] Holthoff H, Egelhaaf SU, Borkovec M, Schurtenberger P, Sticher H. Langmuir 1996;12:5541–9.
[17] Kerker M. The scattering of light and other electromagnetic radiation, physical chemistry. New York: Academic Press; 1969.
[18] Berne BJ, Pecora R. Dynamic Light Scattering. New York: Wiley; 1976.
[19] Koppel DE. J Appl Phys 1972;42(8):3216–25.
[20] Lee SP, Tscharnuter W, Chu B. J Polym Sci 1972;10:2453–9.
[21] Bargeron CB. J Chem Phys 1974;61(5):2134–8.
[22] Koppel DE. J Chem Phys 1972;57(11):4814–20.
[23] von Smoluchowski M. Zeitschrift für Physikalische Chemie 1917;92: 129.
[24] Sandkühler P, Šefčík J, Lattuada M, Wu H, Morbidelli M. AIChE J 2003;49(6):1542–55.
[25] Chen SA, Chang HS. J Polym Sci, Part A—Polym Chem 1990;28(9): 2547–61.
[26] Cardoso AH, Leite CAP, Galembeck F. Langmuir 1998;14(12): 3187–94.
[27] Shirahama H, Suzawa T. J Appl Polym Sci 1984;29(12):3651–61.
[28] Martin-Rodriguez A, Cabrerizo-Vilchez MA, Hidalgo-Alvarez R. Colloids Surf A—Physicochemical Eng Aspects 1996;108(2–3): 263–71.
[29] Fitch RM. Polymer Colloids: a comprehensive introduction. San Diego, CA: Academic Press; 1997.
[30] Kamel A. Ph.D. Thesis, Lehigh University, Bethlehem, PA; 1981.
[31] Min KW, Ray WH. J Macromol Sci—Rev Macromol Chem Phys C 1974;11(2):177–255.
[32] Storti G, Carra S, Morbidelli M, Vita G. J Appl Polym Sci 1989;37(9): 2443–67.
[33] Guillot J. Acta Polymerica 1981;32(10):593.
[34] Nomura M, Fujita K. Makromolekulare Chemie 1985;10/11:25–42.
[35] Kamei S, Okubo M, Matsumoto T. J Polym Sci, Part A—Polym Chem 1986;24(11):3109–16.
[36] Lebduska J, Snuparek J, Kaspar K, Cermak V. J Polym Sci, Part A—Polym Chem 1986;24(4):777–91.